Pump–Probe Detuning Dependence of Four-Wave Mixing Pulse in an SOA

B. F. Kennedy, K. Bondarczuk, and L. P. Barry

***Abstract*—Four-wave mixing (FWM) between 2-ps pulses in a multiquantum-well semiconductor optical amplifier (SOA) is presented. The conjugate pulses are fully characterized using the frequency-resolved optical gating technique. The detuning between the pump and probe is varied, leading to a compression of the FWM signal from 3.71 to 2.77 ps as the detuning is increased from 5 to 25 nm. The output conjugate pulse is always broader than the injected probe signal due to gain saturation effects. A reshaping of the conjugate pulse is also measured. However, large nonlinearities are introduced to the frequency chirp across the pulse for large detunings which may degrade the performance of four-wave-mixing-based all-optical processing applications in SOAs.**

***Index Terms*—Optical pulse measurements, optical signal processing, semiconductor optical amplifiers (SOAs).**

I. Introduction

FOUR-WAVE mixing (FWM) in semiconductor optical amplifiers (SOAs) continues to receive much attention for applications in all-optical processing such as demultiplexing, midspan spectral inversion (MSSI), and differential phase-shift keying (DPSK) wavelength conversion. The latter two applications take advantage of the optical phase conjugate characteristics of the FWM signal [1]–[3]. FWM is sensitive to experimental conditions such as the power level of the pump and probe signals, and the level of bias current supplied to the SOA [4]. This process is also dependent on the pump–probe wavelength separation. Results have been presented measuring the effect on the FWM signal of varying the pump–probe detuning. The majority of these results are limited to analysis of the efficiency and signal-to-background ratio (SBR) [4]. However, Tang and Shore [5] have presented theoretical results, based on pulsed FWM, which show that both the pulsewidth and shape may be controlled by varying the detuning between the pump and probe signals. To date, no experimental results have been presented showing this effect, to the best of the authors' knowledge. Such a technique could be used to simultaneously, and all-optically, control the pulse shape in both time and frequency domains.

Manuscript received June 19, 2007; revised August 23, 20007. This work was supported by Fondo Nacional de Desarrollo Científico y Tecnológico (FONDECYT) Initiation in Research Project.

B. F. Kennedy is with the Engineering Department, Universidad de Santiago, Estacion Central, Chile (e-mail: bkennedy@lauca.usach.cl).

K. Bondarczuk and L. P. Barry are with RINCE, School of Electronic Engineering, Dublin City University, Dublin 9, Ireland (e-mail: liam.barry@dcu.ie).

Color versions of one or more of the figures in this letter are available online at http://ieeexplore.ieee.org.

Digital Object Identifier 10.1109/LPT.2007.909637

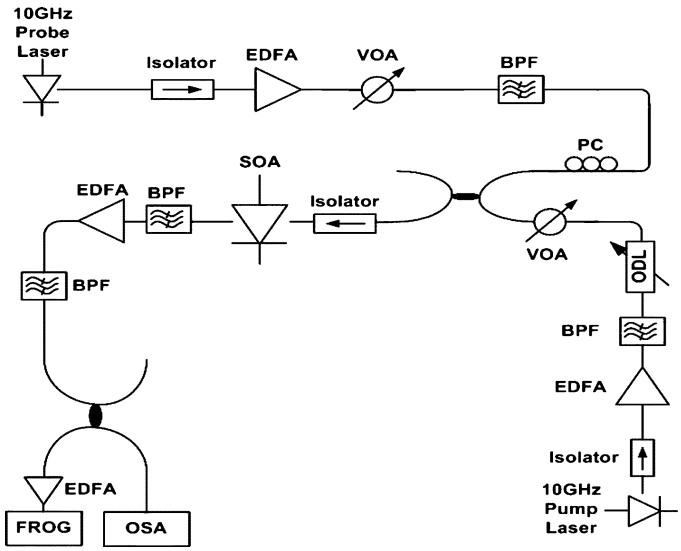

Fig. 1. Experimental setup used to perform FWM in the SOA under test.

Pulse reshaping also affects the phase conjugation characteristics of the FWM signal. This is significant as it would, therefore, affect MSSI and DPSK wavelength conversion based on FWM in the SOA. Experimental results are presented in this letter for the FWM pulse waveform and frequency chirp as a function of detuning. A technique known as frequency-resolved optical gating (FROG) is used which allows for a complete characterization of the conjugate signal. Both pulse compression and reshaping of the FWM signal are measured as the pump–probe detuning is increased. This is attributed to a reduction in the coupling coefficient between the pump and probe signals. However, significant asymmetric behaviour is introduced to the frequency chirp across the FWM signal for large detunings.

II. Experimental Setup

The experimental setup is illustrated in Fig. 1. Two actively mode-locked laser sources were used to produce optical pulses with duration around 2 ps. The repetition rate of both signals was 10 GHz and the wavelength of the pump laser was 1550 nm for each measurement taken. This wavelength is close to the peak gain wavelength of the SOA under test. The wavelength of the probe laser was varied between 1555 and 1575 nm. The signal was amplified and a bandpass filter (BPF) with a bandwidth of 5 nm was used in order to remove amplified spontaneous emission (ASE) introduced by the erbium-doped fiber amplifier (EDFA). The probe signal was then coupled with the pump signal before injection into the SOA. The pump signal was also amplified and filtered by a BPF with a passband of 1 nm before

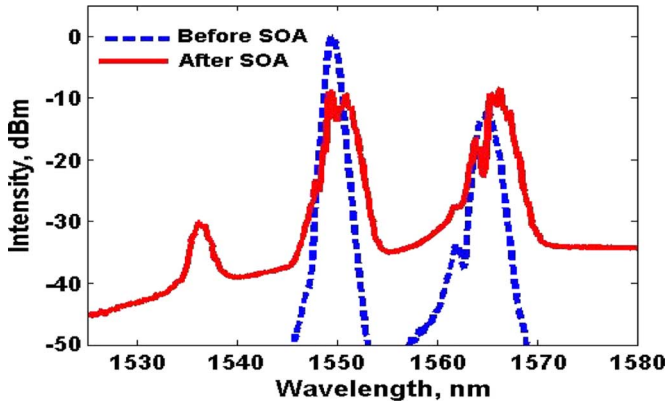

Fig. 2. SOA input and output spectra for 15-nm detuning.

being coupled with the probe. The duration of the pump and probe signals injected into the SOA were 4 and 2 ps, respectively. The broadening of the pump signal caused by the 1-nm BPF was intended, as improved phase conjugation properties have been reported when the pump signal is broader than the probe signal [2]. The optimum average powers of the pump and probe signals were 4 and −10 dBm, respectively. These powers were found by maximizing both the conversion efficiency and SBR using the FWM spectra measured with an optical spectrum analyzer (OSA) of resolution 0.07 nm. Variable optical attenuators (VOAs) were placed in the pump and probe arms to optimize their respective powers. An optical delay line (ODL) was placed in the pump arm of the setup to allow for optimum overlapping of the two signals, to produce the most efficient FWM signal.

The SOA under test was a multiquantum-well device biased at 200 mA, with a peak fiber-to-fiber gain of 25 dB. The length of the active region of the device was 600 μm followed by linearly tapered active regions of 500 μm at each facet [6]. At the output of the SOA, BPFs were used to isolate the FWM component from the output spectrum and to remove ASE introduced by the EDFA. The bandwidth of both BPFs was 2 nm. The FWM component was then examined using second-harmonic generation FROG [7]. The FROG technique generates a three-dimensional spectrogram, which is a time-frequency representation of the pulse. A phase retrieval program is then applied to allow for the electric field of the pulse to be determined, giving the complete temporal and spectral characterization of the pulse [8]. Due to the power requirements of the FROG measurement, an EDFA is used to amplify the pulses before they are input into the FROG measurement system. Low errors of $\approx 4 \times 10^{-5}$ were recorded between the data measured experimentally and those obtained using the retrieval algorithm, which indicates high accuracy [7].

III. Results and Discussion

The spectra measured before and after the SOA are shown in Fig. 2 for a pump–probe detuning of 15 nm. The self-phase modulation introduced to the pump and probe spectra can be clearly seen in this figure. The FWM efficiency, defined as the ratio of the FWM signal intensity to the injected probe intensity, is measured as −18 dB and the SBR is measured as 9 dB

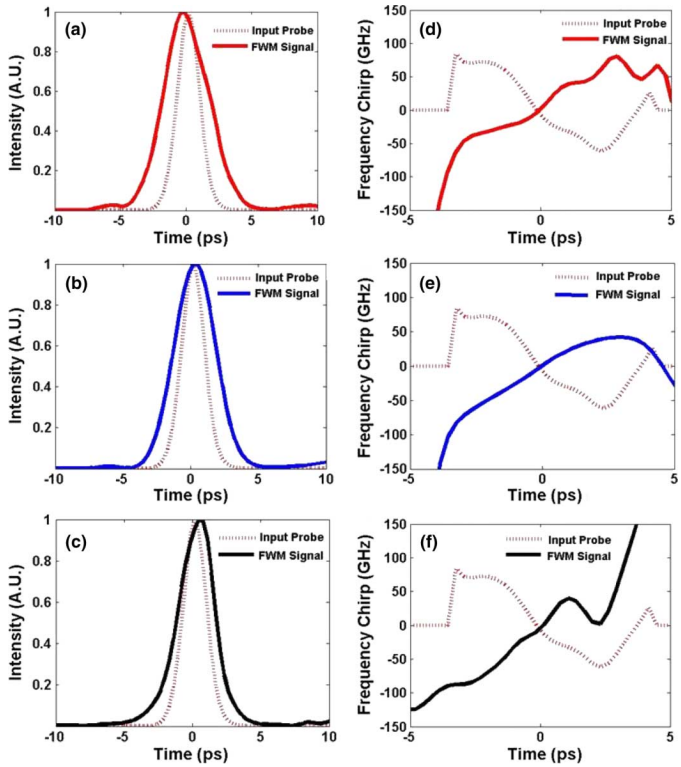

Fig. 3. (a)–(c) Intensity and (d)–(f) frequency chirp of FWM pulses for detunings of 5, 15, and 25 nm, respectively.

from Fig. 2. In comparison, for 5-nm detuning the efficiency is −15.2 dB and the SBR is 12.3 dB. For 25-nm detuning, the efficiency is −25 dB and the SBR is 5.4 dB.

The pump–probe detuning was initially set at 5 nm and the pulse intensity and frequency chirp were measured using FROG. The intensity of the FWM component develops an asymmetric shape, as shown in Fig. 3(a). This asymmetric pulse shape is caused by the high intensity pump signal which is temporally overlapped with the conjugate signal. The leading edge of the pump signal saturates the amplifier and thus reduces the gain available for the trailing edge, causing the rise time to be shorter than the fall time. The peak of the FWM signal shifts towards the leading edge due to the gain suppression caused by the pump signal.

These effects caused by the gain saturation in the device have received much attention in the literature [9]. The FWM pulsewidth for this detuning is 3.71 ps. It would be expected that the FWM signal would be narrower than the probe signal, as it is proportional to $A_0^2 \cdot A_1$, where A_0 and A_1 represent the envelopes of the pump and probe signals, respectively [2], [5]. The broader FWM signal shown in Fig. 3(a) is due to the broadening induced by gain saturation caused by the pump signal [10]. The broadened pump signal at the output of the SOA has a pulsewidth of 5 ps. The probe signal also undergoes broadening and has a pulsewidth of 3.85 ps at the output of the device, for a 5-nm detuning. The output probe pulsewidth does not vary significantly as a function of detuning. The frequency chirp measured across the injected probe signal and the FWM pulse for a detuning of 5 nm is shown in Fig. 3(d). It should be noted that the initial probe chirp is quite large

and may cause transmission limitations. Ideally, the FWM signal chirp should be symmetrical with respect to the injected probe signal chirp. Across the central section of the pulse, near symmetry is achieved. From [9], the temporal variation of the chirp is dependent on the output pulse waveform; therefore, the asymmetry introduced to the trailing edge of the pulse results in corresponding asymmetries in the chirp profile. These asymmetries are significant as they deteriorate the phase conjugation property of the FWM signal with respect to the injected probe signal.

The pump–probe detuning was then increased to 15 nm and the FWM signal was again measured using FROG, as shown in Fig. 3(b). Both a compression and a reshaping of the pulse intensity can be seen in this figure. The pulsewidth is reduced to 3.31 ps for this detuning. The pulse compression is caused by a reduction in the coupling coefficient as the detuning is increased. This effect has been demonstrated theoretically, but not experimentally [5]. The coupling coefficient defines the nonlinear interactions between mixing pulses through temporal gratings formed by the beat frequency. These temporal gratings are defined by several nonlinear processes including carrier depletion, carrier heating and spectral-hole burning which occur on increasingly smaller timescales. Therefore, as the detuning is increased, the gratings are generated over shorter timespans resulting in the conjugate pulse being generated only around the peak intensity of the pump pulse. This has the effect of compressing the FWM pulsewidth. Referring back to the case of 5-nm detuning, it can be seen that the asymmetrical section of the FWM pulse trailing edge occurs away from the peak of the pulse. Therefore, increasing the detuning to 15 nm also has the effect of reshaping the pulse because of the reduction in the coupling coefficient at this larger detuning. This may be seen in Fig. 3(b) as the FWM signal has a more symmetrical shape. The chirp on the FWM signal for a detuning of 15 nm is shown in Fig. 3(e). As is the case for a 5-nm detuning, the chirp is symmetrical with respect to the probe chirp across the central section of the pulse, indicating phase conjugation properties. At 15-nm detuning, the chirp has a linear shape from approximately -3 to 4 ps. The removal of the large asymmetries in this range of the FWM signal causes the FWM signal chirp generated for a 15-nm detuning to be more symmetrical with respect to the injected probe signal than the FWM signal generated for a detuning of 5 nm.

The detuning was increased to 25 nm and the resulting FWM signal intensity and frequency chirp are shown in Fig. 3(c) and (f), respectively. The pulse undergoes further compression; the pulsewidth is 2.77 ps. However, the pulse shape is less symmetrical than is the case for 15-nm detuning. The peak of the pulse shifts towards the trailing edge of the pulse. This indicates that the pump signal is ahead of the probe signal after propagation through the SOA. This is possibly due to a larger shift of the pump signal to the leading edge of the pulse, as reported in [11]. For large detunings, this shift will cause the pump signal to deplete the gain of the device before the leading edge of the probe signal is amplified, resulting in the pulse seen in Fig. 3(c). This result is not in agreement with that reported in [5]. It is believed that this disagreement is due to the large variation in the lengths of the SOA used [11]. The frequency chirp across the FWM pulse is shown in Fig. 3(f). As for detunings of 5 and 15 nm, the chirp across the center of the pulse is symmetric with respect to the input probe signal. However, large nonlinearities are introduced to the chirp away from the peak of the pulse.

IV. Conclusion

Results have been presented demonstrating the effect on FWM pulse intensity and frequency chirp of increasing the pump–probe detuning. A pulse compression of 25% was measured as the detuning was increased from 5 to 25 nm. For all detunings, the FWM signal pulsewidth was larger than the injected probe pulsewidth due to gain saturation effects. Reshaping of the pulse was also measured as a function of detuning. Increasing the detuning from 5 to 15 nm improved the symmetry of the pulse, therefore, causing a more linear frequency chirp and a closer approximation to the phase conjugate of the injected probe signal. An increase in the detuning to 25 nm caused larger pulse compression but also introduced asymmetries which degrade the optical phase conjugation characteristics.

References

[1] N. K. Das, Y. Yamayoshi, T. Kawazoe, and H. Kawaguchi, "Analysis of optical demux characteristics based on four-wave mixing in semiconductor optical amplifiers," *J. Lightw. Technol.*, vol. 19, no. 2, pp. 237–246, Feb. 2001.

[2] N. K. Das, T. Kawazoe, Y. Yamayoshi, and H. Kawaguchi, "Analysis of optical phase-conjugate characteristics of picosecond four-wave mixing signals in semiconductor optical amplifiers," *IEEE J. Quantum Electron.*, vol. 37, no. 1, pp. 55–62, Jan. 2001.

[3] H. Jang, S. Hur, Y. Kim, and J. Jeong, "Theoretical investigation of optical wavelength conversion techniques for DPSK modulation formats using FWM in SOAs and frequency comb in 10 Gb/s transmission systems," *J. Lightw. Technol.*, vol. 23, no. 9, pp. 2638–2646, 2005.

[4] S. Diez, C. Schmidt, R. Ludwig, H. G. Weber, K. Obermann, S. Kindt, I. Koltchanov, and K. Petermann, "Four-wave mixing in semiconductor optical amplifiers for frequency conversion and fast optical switching," *IEEE J. Sel. Topics Quantum Electron.*, vol. 3, no. 5, pp. 1131–1145, Oct. 1997.

[5] J. M. Tang and K. A. Shore, "Characteristics of optical phase conjugation of picosecond pulses in semiconductor optical amplifiers," *IEEE J. Quantum Electron.*, vol. 35, no. 7, pp. 1032–1040, Jul. 1999.

[6] A. E. Kelly, I. F. Lealman, L. J. Rivers, S. D. Perrin, and M. Silver, "Polarisation insensitive, 25 dB gain semiconductor laser amplifier without antireflection coatings," *Electron. Lett.*, vol. 32, no. 19, pp. 1835–1836, Sep. 1996.

[7] R. Trebino, K. W. Long, D. N. Fittinghoff, J. N. Sweetser, M. A. Krumbugel, and B. A. Richman, "Measuring ultrashort laser pulses in the time-frequency domain using frequency resolved optical gating," *Rev. Sci. Instrum.*, vol. 68, pp. 3277–3295, 1997.

[8] D. J. Kane, "Real-time measurement of ultrashort laser pulses using principal component generalized projections," *IEEE J. Sel. Topics Quantum Electron.*, vol. 4, no. 2, pp. 278–284, Mar./Apr. 1998.

[9] G. P. Agrawal and N. A. Olsson, "Self-phase modulation and spectral broadening of optical pulses in semiconductor laser amplifiers," *IEEE J. Quantum Electron.*, vol. 25, no. 11, pp. 2297–2306, Nov. 1989.

[10] A. M. Clarke, M. J. Connelly, P. Anandarajah, L. P. Barry, and D. A. Reid, "Investigation of pulse pedestal and dynamic chirp formation on picosecond pulses after propagation through an SOA," *IEEE Photon. Technol. Lett.*, vol. 17, no. 9, pp. 1800–1802, Sep. 2005.

[11] N. K. Das, Y. Yamayoshi, and H. Kawaguchi, "Analysis of basic four-wave mixing characteristics in a semiconductor optical amplifier by the finite difference beam propagation method," *IEEE J. Quantum Electron.*, vol. 37, no. 1, pp. 55–62, Jan. 2001.